

Kineo-Elasticity and Nonreciprocal Phonons by Rashba-induced Interfacial Spin-Lattice Coupling

Gyungchoon Go* and Se Kwon Kim†

Department of Physics, Korea Advanced Institute of Science and Technology, Daejeon 34141, Korea

We identify a previously unrecognized spin-lattice coupling that is allowed in the presence of broken inversion symmetry that can be considered as a lattice analogue to the electronic Rashba spin-orbit coupling. In the low-frequency regime with magnons integrated out, the interfacial spin-lattice coupling is shown to engender a kineo-elastic term in the phonon Lagrangian that couples the strain on the lattice to its velocity and thereby gives rise to a nonreciprocity in transverse phonon velocity. We further analyze the full magnon-phonon spectrum and uncover directional hybridization and absorption, leading to asymmetric phonon propagation lengths for opposite directions. Our results indicate that such interfacial spin-lattice coupling can serve as an efficient route to achieve nonreciprocal phonon propagation properties in magnetic heterostructures with strong Rashba spin-orbit coupling.

Introduction.—Nonreciprocal propagation of collective excitations has attracted growing interest as a route toward directional control of energy and information flow in condensed-matter systems [1, 2]. In magnetic materials, the breaking of time-reversal and spatial inversion symmetries enables nonreciprocal dynamics of spin waves and phonons [3–14], with implications for magnonics, phononics, and spintronics. For the nonreciprocal propagations several microscopic origins have been reported including long-range dipolar interaction [3–5], Dzyaloshinskii-Moriya interaction [6–9, 15], and magnetoelectric coupling [11–14, 16].

Recently, it has been reported that nonreciprocal propagation can be induced by the coupling between spin and elastic rotation [17]. This spin-vorticity coupling, expressed as $\mathbf{m} \cdot (\nabla \times \dot{\mathbf{u}})$, where \mathbf{m} is the magnetization and $\dot{\mathbf{u}}$ is the lattice displacement, is a universal interaction in bulk magnetic materials that exists independently of spin-orbit interaction or specific crystal symmetries [18–20]. However, while this bulk term originates from the local rotation (vorticity) of the lattice motion, the presence of a physical interface can introduce additional coupling terms. Here, we focus on an interfacial system that emerges specifically when inversion symmetry is broken by the substrate. This symmetry breaking defines a distinguished polar axis \hat{z} , allowing for a gradient-free spin-lattice coupling:

$$\mathcal{L}_{SL} \propto \mathbf{m} \cdot (\hat{z} \times \dot{\mathbf{u}}). \quad (1)$$

which has no counterpart in centrosymmetric bulk systems.

At inversion-broken interfaces, spin-orbit coupling provides a natural microscopic origin for such a velocity-dependent spin-lattice interaction. The Rashba spin-orbit interaction [21] is ubiquitous in magnetic heterostructures and has been extensively studied in the context of current-induced spin torques and chiral magnetic textures [22–27]. However, the lattice has been assumed to be static in the previous works on the Rashba spin-orbit interaction. How the Rashba interaction without the static-lattice assumption couples lattice motion and magnetization dynamics has remained largely unexplored. This raises a fundamental question: whether and how the Rashba spin-orbit interaction can mediate spin-lattice coupling and lead to nonreciprocal phonon dynamics?

In this work, we show that the Rashba spin-orbit interaction, when combined with lattice motion, generates an interfacial spin-lattice coupling that is symmetry-allowed only at inversion-broken interfaces. Within an adiabatic description, the ionic velocity enters the Rashba Hamiltonian as an effective spin-dependent gauge-field term, giving rise to a velocity-dependent coupling between the lattice and the magnetization. We investigate the dynamical consequences of this interfacial coupling for phonon and magnon-phonon excitations. In the low-frequency regime, where the magnon degrees of freedom can be integrated out, the interfacial spin-lattice coupling produces a kineo-elastic term which couples the lattice strain with its velocity [28] in the effective phonon Lagrangian. This term is odd under momentum reversal and leads to a nonreciprocity in transverse phonon propagation.

Beyond the low-frequency regime, we analyze the full magnon-phonon spectrum and uncover a strong directional hybridization between transverse phonons and magnons. The hybridization is enhanced for one propagation direction while being suppressed for the opposite direction, leading to a marked asymmetry in phonon absorption by magnons. Consequently, phonons propagating in one direction are efficiently absorbed over a short distance, whereas long-range phonon propagation is preserved in the opposite direction. These effects provide clear dynamical signatures of the Rashba-induced interfacial spin-lattice coupling. Our results indicate that interfacial spin-lattice coupling can play an important role in controlling phonon propagation properties in magnetic heterostructures with strong Rashba spin-orbit coupling.

Interfacial spin-lattice coupling.—We consider a system characterized by a parabolic band approximation with an effective mass m_{eff} , such that the momentum is given by $\mathbf{p} = m_{\text{eff}}\mathbf{v}$, where \mathbf{v} is the group velocity of the electron. The standard Rashba spin-orbit energy for a two-dimensional system with broken inversion symmetry along \hat{z} is expressed as [21]: $H_R = \frac{\alpha_R}{\hbar} (\boldsymbol{\sigma} \times \mathbf{p}) \cdot \hat{z}$, where α_R is the Rashba coefficient, $\boldsymbol{\sigma}$ is the vector of Pauli matrices representing the electron spin.

In the presence of moving lattice displacement $\mathbf{u}(t)$, electrons experience a momentum shift $\mathbf{p} \rightarrow \mathbf{p} + \delta\mathbf{p}$ via the lattice-tracking effect. Within the wave-packet formalism, this induced shift is given by $\delta\mathbf{p} = -(m_{\text{eff}} - m_e)\dot{\mathbf{u}}$ [29–31], where m_e is bare electron mass. This term reflects the incomplete

cancellation between the inertial effect and the lattice-potential drag effect, and is generally present in lattice systems where $m_{\text{eff}} \neq m_e$. By substituting this into the Rashba Hamiltonian, we obtain $H_R = H_R^0 + H_{SL}$ where H_R^0 is the conventional Rashba term and $H_{SL} = -\Lambda_{SL}\boldsymbol{\sigma} \cdot (\hat{z} \times \dot{\mathbf{u}})$ describes the interfacial spin-lattice coupling, with the coupling constant defined as: $\Lambda_{SL} = \alpha_R(m_{\text{eff}} - m_e)/\hbar$.

In the limit of strong exchange interaction, where the electron spin dynamics is dominated by the exchange field, the spin expectation value is effectively locked to the local magnetization direction \mathbf{m} . By identifying $\boldsymbol{\sigma} \simeq -\mathcal{P}\mathbf{m}$, where \mathcal{P} denotes the spin polarization, we arrive at our foundational equation for the energy density describing the effective interfacial spin-lattice coupling:

$$\mathcal{H}_{SL} = \lambda_{SL}\mathbf{m} \cdot (\hat{z} \times \dot{\mathbf{u}}), \quad (2)$$

where $\lambda_{SL} = n\mathcal{P}\Lambda_{SL}$ is the renormalized coupling constant, with n denoting the density of magnetic moments. This velocity-dependent interaction provides a hitherto unrecognized symmetry-allowed coupling between magnetic order and lattice dynamics at inversion-broken interfaces and it is our first main result.

For a localized acoustic wave at the interface, characterized by a displacement field $u \propto e^{-z/l}$, where l is the penetration depth of the acoustic wave, the effect of our interaction resembles that of the spin-vorticity coupling [18–20]: $\mathcal{H}_{sv} = nS\mathbf{m} \cdot (\nabla \times \dot{\mathbf{u}})/2 = \lambda_{sv}\mathbf{m} \cdot (\hat{z} \times \dot{\mathbf{u}})$, where $\lambda_{sv} = nS/(2l)$, but the two are from different mechanisms and therefore they can differ in magnitude. In particular, since our interaction comes from the interfacial spin-orbit coupling, unlike the spin-vorticity coupling that is agnostic to it, the former can be much stronger than the latter in systems with strong interfacial spin-orbit coupling. For a typical set of parameters— $\mathcal{P} = 0.5$, $\alpha_R = 2 \text{ eV}\text{\AA}$ [22], $m_{\text{eff}} = 1.5 m_e$, $l = 2 \mu\text{m}$, and $S = \hbar$ —we obtain a ratio $\lambda_{SL}/\lambda_{sv} \approx 2.5 \times 10^3$. This significant enhancement indicates that the Rashba-induced spin-lattice coupling can be much more potent than the conventional spin-vorticity effect in interfacial systems with broken inversion symmetry. To explore the dynamical consequences of this interaction, we now investigate its impact on the nonreciprocal phonon spectrum and the nature of magnon-phonon hybridization.

Minimal model.—We consider a ferromagnetic thin film in the xy -plane, bonded to a substrate below ($z < 0$), which breaks inversion symmetry ($z \rightarrow -z$). As shown in Fig. 1, we take the equilibrium magnetization to lie in the xz -plane, $\mathbf{m}_0 = (\cos \theta, 0, \sin \theta)$, and describe small transverse fluctuations as $\delta\mathbf{m} \approx \mathbf{R}(\theta)(m'_x, m'_y, 0)$ with $|m'_{x,y}| \ll 1$, where $\mathbf{R}(\theta)$ is a rotation matrix that aligns the local quantization axis \hat{z}' with the equilibrium direction. Hereafter, we drop the prime notation and denote the magnetization fluctuations simply by m_x and m_y . The in-plane lattice displacement is defined as $\mathbf{u} = (u_x, u_y)$ with the corresponding strain tensor $u_{ij} = (\partial_i u_j + \partial_j u_i)/2$.

The quadratic Lagrangian density of the system is given by

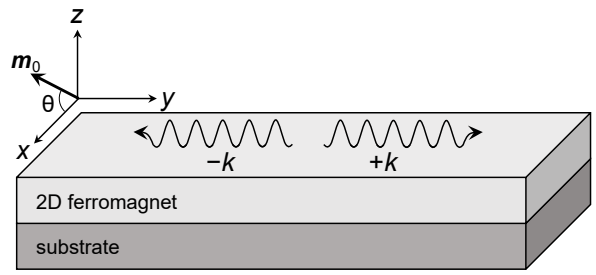


FIG. 1. **Schematic of a 2D ferromagnet on a substrate used for the model.** The system consists of a two-dimensional ferromagnetic film in the xy -plane bonded to a substrate that breaks inversion symmetry along the \hat{z} direction. The equilibrium magnetization \mathbf{m}_0 lies in the xz -plane with an angle θ from the x -axis, given by $\mathbf{m}_0 = (\cos \theta, 0, \sin \theta)$. The wavy arrows represent the propagation of acoustic waves (phonons) along the \hat{y} direction with wavevectors $\pm k$.

$$\mathcal{L} = \mathcal{L}_{\text{ph}} + \mathcal{L}_{\text{m}} + \mathcal{L}_{\text{m-ph}}$$

$$\begin{aligned} \mathcal{L} = & \underbrace{\frac{\rho}{2}\dot{\mathbf{u}}^2 - \frac{1}{2}\mathbf{u} \cdot \mathbf{D} \cdot \mathbf{u}}_{\mathcal{L}_{\text{ph}}} \\ & + \underbrace{\frac{\rho_s}{2}\epsilon_{ij}m_i\dot{m}_j - \frac{1}{2}[\Delta(m_i)^2 + A_{\text{ex}}(\nabla m_i)^2]}_{\mathcal{L}_{\text{m}}} \\ & - \underbrace{\lambda_{SL}(m_y\dot{u}_x - \sin \theta m_x\dot{u}_y)}_{\mathcal{L}_{\text{SL}}} - \underbrace{2b_2 \cos \theta m_y u_{xy}}_{\mathcal{L}_{\text{me}}} \end{aligned} \quad (3)$$

where the Einstein summation convention is applied to repeated indices $i, j \in \{x, y\}$. Here, ρ is the mass density, $\mathbf{D}_{ij} \equiv (\lambda_L + \mu)\partial_i\partial_j + \mu\nabla^2\delta_{ij}$ is the isotropic elastic operator with Lamé coefficients (λ_L, μ). In the magnon sector \mathcal{L}_{m} , ρ_s is the spin density, ϵ_{ij} is the 2D Levi-Civita symbol dictating gyroscopic precession, $\Delta (= \gamma\rho_s B_{\text{eff}})$ is the magnonic gap, and A_{ex} is the exchange stiffness. The interaction term $\mathcal{L}_{\text{m-ph}} = \mathcal{L}_{\text{SL}} + \mathcal{L}_{\text{me}}$ includes the interfacial spin-lattice coupling and the conventional magnetoelastic interaction with a coefficient b_2 [16].

For the numerical analysis throughout this study, we adopt a set of material parameters representative of typical interfacial ferromagnetic systems such as Pt/Co. Specifically, we take $m_{\text{eff}} = 1.5 m_e$, $\alpha_R = 2 \text{ eV}\text{\AA}$, $\mathcal{P} = 0.5$ [22]. For the elastic sector, we use $\rho = 8.8 \text{ g/cm}^3$, $\mu = 82 \text{ GPa}$ and $\lambda = 135 \text{ GPa}$ [32]. The magnetic parameters are taken as $\rho_s = 7.2 \times 10^{28} \hbar/\text{m}^3$ and $A_{\text{ex}} = 2.1 \times 10^{11} \text{ J/m}$ [33]. Finally, the magnetoelastic coupling constant is set to $b_2 = -1.62 \times 10^8 \text{ erg/cm}^3$ [34].

Effective phonon model: kineo-elastic coupling.—In the adiabatic regime $\rho_s|\omega|, Ak^2 \ll \Delta$, the massive magnon fields m_i can be integrated out to quadratic order. To leading order in Δ^{-1} , we derive the effective phonon Lagrangian $\mathcal{L}_{\text{eff}} =$

$\mathcal{L}_{\text{ph}} + \delta\mathcal{L}$, where the correction term $\delta\mathcal{L}$ is given by:

$$\delta\mathcal{L} \simeq \frac{(\lambda_{SL}\dot{u}_x + 2b_2 \cos \theta u_{xy})^2 + (\lambda_{SL} \sin \theta \dot{u}_y)^2}{2\Delta} - \underbrace{\eta \dot{u}_x u_{xy} + \frac{\lambda_{SL}^2}{2\Delta} (\dot{u}_x^2 + \sin^2 \theta \dot{u}_y^2) + \frac{2b_2^2 \cos^2 \theta}{\Delta} u_{xy}^2}_{\mathcal{L}_{\text{ke}}}, \quad (4)$$

with the coefficient $\eta \equiv 2\lambda_{SL}b_2 \cos \theta / \Delta$. The last two terms in Eq. (4) simply renormalize the inertia of $u_{x,y}$ and the shear modulus; however, the term \mathcal{L}_{ke} introduces a distinct mixed structure. This term corresponds to the *kineo-elastic coupling*, which couples the lattice strain to its velocity [28]. The term \mathcal{L}_{ke} is: (i) linear in ∂_i , hence odd under $\mathbf{k} \rightarrow -\mathbf{k}$; (ii) linear in ∂_t , hence reactive (nondissipative); (iii) allowed only when the equilibrium magnetization breaks the in-plane rotational symmetry ($\cos \theta \neq 0$).

We now analyze the phonon modes of $\mathcal{L}_{\text{ph}} + \mathcal{L}_{\text{ke}}$. Note that in the following analysis, we focus on the effects of the kineo-elastic term \mathcal{L}_{ke} and ignore the renormalization of the inertia and the shear modulus, which are proportional to λ_{SL}^2 and b_2^2 . For plane waves $\mathbf{u}(\mathbf{r}, t) = \mathbf{u}e^{i(\mathbf{k} \cdot \mathbf{r} - \omega t)}$, the equations of motion take the matrix form:

$$[\rho\omega^2 \mathbf{1} - \omega \mathbf{K}(\mathbf{k}) - \mathbf{D}(\mathbf{k})] \mathbf{u} = 0, \quad (5)$$

where $D_{ij}(\mathbf{k}) = (\lambda_L + \mu)k_i k_j + \mu k^2 \delta_{ij}$, and the kineo-elastic contribution $\mathbf{K}(\mathbf{k})$ is given by:

$$\mathbf{K}(\mathbf{k}) = \eta \begin{pmatrix} k_y & k_x/2 \\ k_x/2 & 0 \end{pmatrix}. \quad (6)$$

Because $\mathbf{K}(\mathbf{k})$ is odd in \mathbf{k} , the phonon dispersions obtained from Eq. (5) generally satisfy $\omega_\alpha(\mathbf{k}) \neq \omega_\alpha(-\mathbf{k})$. This nonreciprocal phonon modes are most transparent along the propagation direction $\mathbf{k} = k\hat{\mathbf{y}}$ (where $k_x = 0$), where longitudinal (u_y) and transverse (u_x) motions decouple. Keeping the leading order in η , the dispersions of the transverse and longitudinal modes are given by:

$$\omega_T(k) \simeq c_T |k| + \frac{\eta}{2\rho} k, \quad \omega_L(k) = c_L |k|, \quad (7)$$

where $c_T = \sqrt{\mu/\rho}$ and $c_L = \sqrt{\lambda_L + 2\mu/\rho}$. Equation (7) is explicitly nonreciprocal for transverse mode $\omega_T(k) \neq \omega_T(-k)$ while the longitudinal mode is reciprocal $\omega_L(k) = \omega_L(-k)$. Consequently, the group velocity of the transverse phonon mode differs for right- and left-moving waves by $\Delta v \equiv v_g(k > 0) - v_g(k < 0) = \eta/\rho$. This is our second main result: the interfacial spin-lattice coupling [Eq. (2)] induces the kineo-elastic coupling [Eq. (4)] between the lattice strain and the lattice velocity and thereby gives rise to the nonreciprocity in the transverse phonon transport [Eq. (7); Fig. 2].

Away from high-symmetry lines, $\mathbf{K}(\mathbf{k})$ mixes longitudinal and transverse polarizations at linear order in η , producing direction-dependent elliptic polarizations. For small $|\eta|$, a

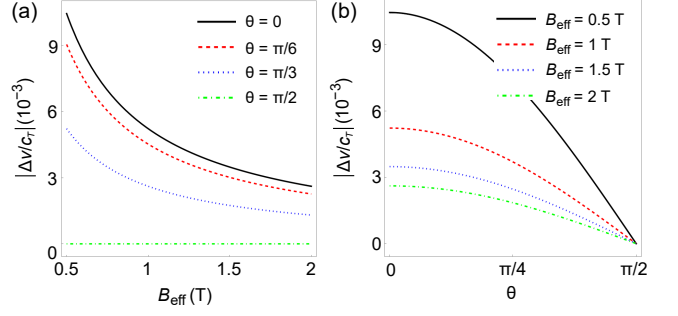


FIG. 2. **Nonreciprocity of the phonon velocity.** The relative velocity asymmetry $|\Delta v/c_T|$ is shown as a function of (a) the effective magnetic field B_{eff} and (b) the magnetization orientation θ .

compact perturbative expression for the leading odd-in- k shift of a mode $\alpha \in \{L, T\}$ is derived from Eq. (5) as:

$$\delta\omega_\alpha(k) = -\frac{(\mathbf{u}_\alpha^{(0)})^T \mathbf{K}(\mathbf{k}) \mathbf{u}_\alpha^{(0)}}{2\rho}, \quad (8)$$

where $\mathbf{u}_\alpha^{(0)}$ is the unperturbed eigenvector. Together with Eq. (6), this result indicates that nonreciprocity is maximized for propagation directions and polarizations with a large u_x component and a finite k_y component, which is a direct consequence of the interfacial axis $\hat{\mathbf{z}}$ and magnetization direction \mathbf{m}_0 .

In Fig. 2, we show the nonreciprocity of the phonon velocity. The nonreciprocity is maximal for $\theta = 0$ ($\mathbf{m} = \hat{\mathbf{x}}$), is reduced at intermediate angles, and vanishes when the magnetization is perpendicular to the propagation direction ($\theta = \pi/2$; $\mathbf{m} = \hat{\mathbf{z}}$). We note that the nonreciprocity discussed here shares certain similarities with the nonreciprocal propagation arising from magnetoelastic interactions reported previously [11, 14]. However, an important distinction is that our effective phonon model is formulated in a regime far away from the magnon–phonon resonance, where the magnon degrees of freedom can be integrated out. Despite being off resonance, the resulting nonreciprocity can be substantially larger than the velocity asymmetry, typically of order $\Delta v/v_0 \sim 10^{-5}$, expected from the magnetoelastic interactions [11, 14], depending on the strength of the Rashba interaction in our model. A full magnon–phonon band structure including the resonance region, and the resulting nonreciprocity, will be discussed in the following section.

Directional magnon-phonon coupling.—Here we analyze the both magnon and phonon modes of Eq. (3). The matrix form of the equations of motion is:

$$[\rho\omega^2 \mathbb{P}_{\text{ph}} - i\omega \rho_s \mathbb{P}_{\text{m}} \epsilon - \mathbb{D}(\mathbf{k}) + \mathbb{K}(\mathbf{k}, \omega)] \Psi = 0, \quad (9)$$

where $\Psi = (u_x, u_y, m_x, m_y)$. Here $\mathbb{P}_{\text{ph}} = \text{diag}(1, 1, 0, 0)$ and $\mathbb{P}_{\text{m}} = \text{diag}(0, 0, 1, 1)$ are projection operators onto the phonon and magnon subspaces, respectively, and ϵ is the 2D Levi-Civita tensor acting in the magnon space. The matrix $\mathbb{D}(\mathbf{k})$ is dynamical matrix including bare phonon and magnon

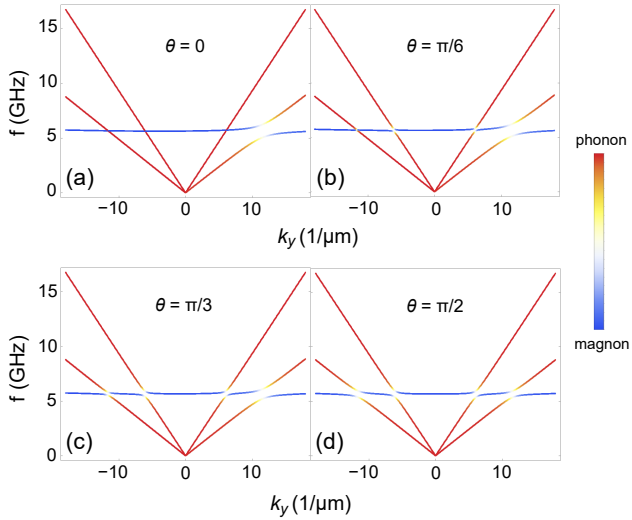


FIG. 3. **Directional magnon–phonon hybridization.** Dispersion relations of the magnon-phonon spectrum as a function of the wave vector k_y , taken along the propagation direction $\mathbf{k} = k_y \hat{y}$, for different magnetization orientations: (a) $\theta = 0$, (b) $\theta = \pi/6$, (c) $\theta = \pi/3$, and (d) $\theta = \pi/2$. The color scale indicates the phonon (red) and magnon (blue) character of each hybridized mode. An effective magnetic field $B_{\text{eff}} = 0.2$ T is used.

sectors, while the antisymmetric matrix $\mathbb{K}(\mathbf{k}, \omega)$ describes the magnon-phonon couplings due to the magnetoelastic and interfacial spin-lattice couplings [see Supplemental Material for full expressions of $\mathbb{D}(\mathbf{k})$ and $\mathbb{K}(\mathbf{k}, \omega)$].

Fig. 3 show that the magnon-phonon spectrum along the propagation direction $\mathbf{k} = k_y \hat{y}$ ($k_x = 0$) for different magnetization orientations. We observe a pronounced directional hybridization between the transverse phonon and the magnon for small θ , where the anticrossing gap induced by the magnon–phonon coupling is asymmetric under $k_y \rightarrow -k_y$. This directionality is gradually suppressed as the magnetization is rotated and vanishes at $\theta = \pi/2$. In contrast, no such asymmetric hybridization is observed between the longitudinal phonon and the magnon. This behavior can be traced back to the structure of the matrix \mathbb{K} . For $k_x = 0$, the only nonvanishing elements of the matrix \mathbb{K} are $\mathbb{K}_{(u_x, m_y)}$ and $\mathbb{K}_{(u_y, m_x)}$ (see Supplemental Material). Because the hybridization between transverse phonon (u_x) and the magnon is governed by $\mathbb{K}_{(u_x, m_y)} = i(\omega\lambda_{\text{SL}} - b_2 \cos \theta k_y)$, the magnetoelastic coupling and interfacial spin-lattice couplings compete as a functions of k_y resulting in directional hybridization. By contrast, the hybridization between longitudinal phonon (u_y) and the magnon, $\mathbb{K}_{(u_y, m_x)} = -i\omega\lambda_{\text{SL}} \sin \theta$, is mediated solely by the interfacial spin-lattice coupling. This is our third main result: the interfacial spin-lattice coupling [Eq. (2)] leads to the direction-dependent hybridization between magnons and phonons (Fig. 3), engendering nonreciprocal phonon absorption by magnons (Fig. 4).

The asymmetric magnon-phonon coupling give rise to nonreciprocal phonon absorption by magnons. To quan-

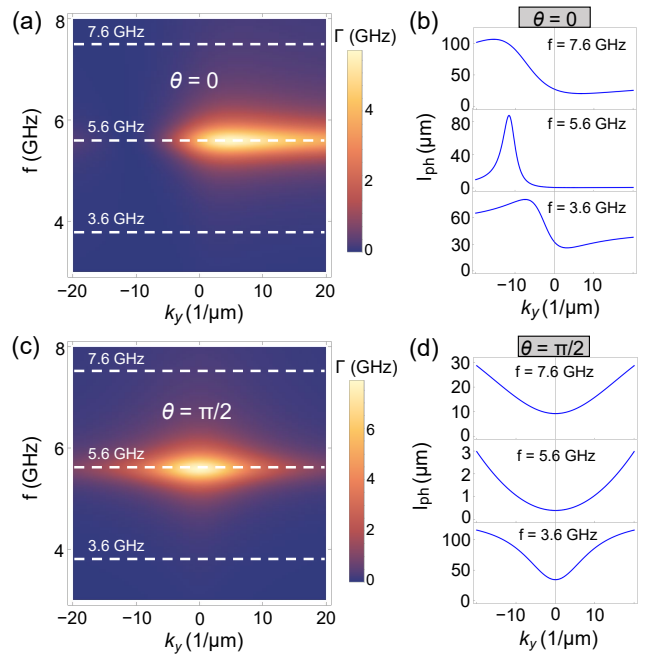


FIG. 4. **Nonreciprocal phonon absorption and propagation length.** The absorption rate of phonon energy by magnons, $\Gamma_{\text{m-ph}}$, is shown as a function of the phonon wave vector k_y for different phonon frequencies for (a) $\theta = 0$ and (c) $\theta = \pi/2$. Panels (b) and (d) display the corresponding phonon propagation length for (b) $\theta = 0$ and (d) $\theta = \pi/2$. An effective magnetic field $B_{\text{eff}} = 0.2$ T, Gilbert damping $\alpha = 0.05$, and $Q = 1000$ are used. The data are obtained for $k_x = 0$ with equal amplitudes of the in-plane phonon displacements, $u_x = u_y$.

tify this effect, we compute the absorption rate of phonon energy transferred to magnons, $\Gamma_{\text{m-ph}} = \Delta P / \langle \mathcal{E}_{\text{ph}} \rangle$, where $\Delta P = \gamma \rho_s \langle \mathbf{B}_{\text{m-ph}}(t) \cdot \dot{\mathbf{m}}(t) \rangle$ and $\langle \mathcal{E}_{\text{ph}} \rangle$ are the time-averaged absorption power and phonon energy, respectively. Here, $\mathbf{B}_{\text{m-ph}} = \frac{1}{\gamma \rho_s} \frac{\partial \mathcal{L}_{\text{m-ph}}}{\partial \mathbf{m}}$ is the effective magnetic field induced by the magnon-phonon couplings (see Supplemental Material). As shown in Fig. 4(a) and (c), the resulting absorption rate exhibits strong nonreciprocity for $\theta = 0$ case while it becomes fully reciprocal at $\theta = \pi/2$. Figures 4(b) and (d) display the corresponding phonon propagation length, $l_{\text{ph}} \sim v_g / (\Gamma_0 + \Gamma_{\text{m-ph}})$, where $\Gamma_0 = \omega/Q$ and Q denotes the quality factor characterizing the intrinsic phonon attenuation. A pronounced directional contrast in the propagation length is observed for $\theta = 0$, whereas the propagation lengths for opposite directions become identical at $\theta = \pi/2$. For simplicity, we assume $k_x = 0$ and equal amplitudes of the in-plane phonon displacements, $u_x = u_y$, in the numerical calculations. We emphasize, however, that the resulting nonreciprocal phonon absorption is a generic feature of transverse phonons for $\theta \neq \pi/2$.

Discussion.—We have shown that the Rashba spin–orbit interaction, together with lattice motion, gives rise to an interfacial spin–lattice coupling. The resulting velocity-dependent coupling between the lattice and the magnetization constitutes

a hitherto unrecognized, symmetry-allowed interaction at interfaces lacking inversion symmetry. In the low-frequency limit, by integrating out the magnons, we obtained an effective phonon model with a kineo-elastic coupling that is linear in both the time derivative and the wave vector. This kineo-elastic term leads to a finite velocity asymmetry of transverse phonons, whose magnitude can exceed by orders of magnitude the velocity asymmetry $\Delta v/v_0 \sim 10^{-5}$ typically expected from conventional magnetoelastic interactions. Beyond low-frequency limit, we investigated the full magnon-phonon spectrum, which exhibits a directional magnon-phonon coupling: the coupling is strong for one propagation direction, while it is strongly suppressed for the opposite direction. Consequently, phonons propagating in one direction are efficiently absorbed into magnons over a short distance, whereas long-range phonon propagation is preserved in the opposite direction.

Our results suggest an experimentally accessible route. The predicted nonreciprocal velocity shift and asymmetric phonon absorption can be probed using shear-horizontal surface acoustic waves (Love waves), which possess an in-plane transverse lattice displacement component [35, 36] at inversion-broken interfaces. The dependence on the magnetization orientation provides a clear experimental knob to disentangle the Rashba-induced contribution from conventional magnetoelastic effects. A fully quantitative comparison with experiments will require a detailed characterization of the interfacial Rashba strength and the phonon mode profiles.

Finally, the interfacial spin-lattice coupling identified here may have broader implications. In particular, our results point to a wide range of phononic transport phenomena and possible nonlinear extensions, such as nonreciprocal thermal transport. In addition, the odd-in- k dynamical term may imply a non-trivial Berry curvature of phonon and magnon-phonon bands, suggesting controllable thermal Hall responses in interfacial magnetic systems. These directions remain interesting avenues for future studies.

ACKNOWLEDGEMENT

We thank Daniel E. Parker for insightful discussions. G.G. was supported by the National Research Foundation of Korea (NRF-2022R1C1C2006578). S.K.K. was supported by Brain Pool Plus Program through the National Research Foundation of Korea funded by the Ministry of Science and ICT (2020H1D3A2A03099291).

- [2] S.-W. Cheong, D. Talbayev, V. Kiryukhin, and A. Saxena, Broken symmetries, non-reciprocity, and multiferroicity, *npj Quantum Mater.* **3**, 19 (2018).
- [3] M. Jamali, J. H. Kwon, S.-M. Seo, K.-J. Lee, and H. Yang, Spin wave nonreciprocity for logic device applications, *Sci. Rep.* **3**, 3160 (2013).
- [4] M. Kostylev, Non-reciprocity of dipole-exchange spin waves in thin ferromagnetic films, *J. Appl. Phys.* **113**, 053907 (2013).
- [5] T. An, V. I. Vasyuchka, K. Uchida, A. V. Chumak, K. Yamaguchi, K. Harii, J. Ohe, M. B. Jungfleisch, Y. Kajiwara, H. Adachi, B. Hillebrands, S. Maekawa, and E. Saitoh, Unidirectional spin-wave heat conveyer, *Nat. Mater.* **12**, 549 (2013).
- [6] Y. Iguchi, S. Uemura, K. Ueno, and Y. Onose, Nonreciprocal magnon propagation in a noncentrosymmetric ferromagnet LiFe_5O_8 , *Phys. Rev. B* **92**, 184419 (2015).
- [7] S. Seki, Y. Okamura, K. Kondou, K. Shibata, M. Kubota, R. Takagi, F. Kagawa, M. Kawasaki, G. Tatara, Y. Otani, and Y. Tokura, Magnetochiral nonreciprocity of volume spin wave propagation in chiral-lattice ferromagnets, *Phys. Rev. B* **93**, 235131 (2016).
- [8] T. J. Sato, D. Okuyama, T. Hong, A. Kikkawa, Y. Taguchi, T.-h. Arima, and Y. Tokura, Magnon dispersion shift in the induced ferromagnetic phase of noncentrosymmetric mnsi, *Phys. Rev. B* **94**, 144420 (2016).
- [9] T. Nomura, X.-X. Zhang, S. Zherlitsyn, J. Wosnitza, Y. Tokura, N. Nagaosa, and S. Seki, Phonon magnetochiral effect, *Phys. Rev. Lett.* **122**, 145901 (2019).
- [10] Y. Hirokane, Y. Nii, H. Masuda, and Y. Onose, Nonreciprocal thermal transport in a multiferroic helimagnet, *Sci. Adv.* **6**, eabd3703 (2020).
- [11] R. Sasaki, Y. Nii, Y. Iguchi, and Y. Onose, Nonreciprocal propagation of surface acoustic wave in Ni/LiNbO_3 , *Phys. Rev. B* **95**, 020407 (2017).
- [12] S. Tateno and Y. Nozaki, Highly Nonreciprocal Spin Waves Excited by Magnetoelastic Coupling in a Ni/Si Bilayer, *Phys. Rev. Appl.* **13**, 034074 (2020).
- [13] J. Puebla, M. Xu, B. Rana, K. Yamamoto, S. Maekawa, and Y. Otani, Acoustic ferromagnetic resonance and spin pumping induced by surface acoustic waves, *J. Phys. D: Appl. Phys.* **53**, 264002 (2020).
- [14] P. Rovillain, J.-Y. Duquesne, L. Christienne, M. Eddrief, M. G. Pini, A. Rettori, S. Tacchi, and M. Marangolo, Impact of spin-wave dispersion on surface-acoustic-wave velocity, *Phys. Rev. Appl.* **18**, 064043 (2022).
- [15] T. Moriya, Anisotropic superexchange interaction and weak ferromagnetism, *Phys. Rev.* **120**, 91 (1960).
- [16] C. Kittel, Physical theory of ferromagnetic domains, *Rev. Mod. Phys.* **21**, 541 (1949).
- [17] M. Xu, K. Yamamoto, J. Puebla, K. Baumgaertl, B. Rana, K. Miura, H. Takahashi, D. Grundler, S. Maekawa, and Y. Otani, Nonreciprocal surface acoustic wave propagation via magneto-rotation coupling, *Sci. Adv.* **6**, eabb1724 (2020).
- [18] M. Matsuo, J. Ieda, K. Harii, E. Saitoh, and S. Maekawa, Mechanical generation of spin current by spin-rotation coupling, *Phys. Rev. B* **87**, 180402 (2013).
- [19] M. Matsuo, E. Saitoh, and S. Maekawa, Spin-mechatronics, *J. Phys. Soc. Jpn.* **86**, 011011 (2017).
- [20] T. Funato and M. Matsuo, Spin elastodynamic motive force, *Phys. Rev. Lett.* **128**, 077201 (2022).
- [21] Y. A. Bychkov and E. I. Rashba, Oscillatory effects and the magnetic susceptibility of carriers in inversion layers, *J. Phys. C: Solid State Phys.* **17**, 6039 (1984).
- [22] I. Mihai Miron, G. Gaudin, S. Auffret, B. Rodmacq, A. Schuhl, S. Pizzini, J. Vogel, and P. Gambardella, Current-driven spin torque induced by the Rashba effect in a ferromagnetic metal

* gyungchoon@gmail.com

† sekwonkim@kaist.ac.kr

[1] Y. Tokura and N. Nagaosa, Nonreciprocal responses from noncentrosymmetric quantum materials, *Nat. Commun.* **9**, 3740 (2018).

layer, *Nat. Mater.* **9**, 230 (2010).

[23] K. Garello, I. M. Miron, C. O. Avci, F. Freimuth, Y. Mokrousov, S. Blügel, S. Auffret, O. Boulle, G. Gaudin, and P. Gambardella, Symmetry and magnitude of spin–orbit torques in ferromagnetic heterostructures, *Nat. Nanotechnol.* **8**, 587 (2013).

[24] H. Kurebayashi, J. Sinova, D. Fang, A. C. Irvine, T. D. Skinner, J. Wunderlich, V. Novák, R. P. Campion, B. L. Gallagher, E. K. Vehstedt, L. P. Zárbo, K. Výborný, A. J. Ferguson, and T. Jungwirth, An antidamping spin–orbit torque originating from the Berry curvature, *Nat. Nanotechnol.* **9**, 211 (2014).

[25] K.-W. Kim, H.-W. Lee, K.-J. Lee, and M. D. Stiles, Chirality from interfacial spin-orbit coupling effects in magnetic bilayers, *Phys. Rev. Lett.* **111**, 216601 (2013).

[26] H. Yang, G. Chen, A. A. C. Cotta, A. T. N'Diaye, S. A. Nikolaev, E. A. Soares, W. A. A. Macedo, K. Liu, A. K. Schmid, A. Fert, and M. Chshiev, Significant Dzyaloshinskii–Moriya interaction at graphene–ferromagnet interfaces due to the Rashba effect, *Nat. Mater.* **17**, 605 (2018).

[27] H. C. Koo, S. B. Kim, H. Kim, T.-E. Park, J. W. Choi, K.-W. Kim, G. Go, J. H. Oh, D.-K. Lee, E.-S. Park, I.-S. Hong, and K.-J. Lee, Rashba effect in functional spintronic devices, *Adv. Mater.* **32**, 2002117 (2020).

[28] J. Dong, O. E. Sommer, T. Soejima, D. E. Parker, and A. Vishwanath, Phonons in electron crystals with berry curvature, *Proc. Natl. Acad. Sci. U.S.A.* **122**, e2515532122 (2025).

[29] T. Holstein, Theory of ultrasonic absorption in metals: the collision-drag effect, *Phys. Rev.* **113**, 479 (1959).

[30] F. S. Khan and P. B. Allen, Deformation potentials and electron–phonon scattering: Two new theorems, *Phys. Rev. B* **29**, 3341 (1984).

[31] G. Sundaram and Q. Niu, Wave-packet dynamics in slowly perturbed crystals: Gradient corrections and berry-phase effects, *Phys. Rev. B* **59**, 14915 (1999).

[32] H. J. McSkimin, Measurement of the Elastic Constants of Single Crystal Cobalt, *J. Appl. Phys.* **26**, 406 (1955).

[33] C. Eyrich, W. Hüttema, M. Arora, E. Montoya, F. Rashidi, C. Burrowes, B. Kardasz, E. Girt, B. Heinrich, O. N. Mryasov, M. From, and O. Karis, Exchange stiffness in thin film Co alloys, *J. Appl. Phys.* **111**, 07C919 (2012).

[34] T. Gutjahr-Löser, D. Sander, and J. Kirschner, Magnetoelastic coupling in Co thin films on W(0 0 1), *J. Magn. Magn. Mater.* **220**, 1 (2000).

[35] L. Dreher, M. Weiler, M. Pernpeintner, H. Huebl, R. Gross, M. S. Brandt, and S. T. B. Goennenwein, Surface acoustic wave driven ferromagnetic resonance in nickel thin films: Theory and experiment, *Phys. Rev. B* **86**, 134415 (2012).

[36] Y. Yang, L. Zhao, D. Yi, T. Xu, Y. Chai, C. Zhang, D. Jiang, Y. Ji, D. Hou, W. Jiang, J. Tang, P. Yu, H. Wu, and T. Nan, Acoustic-driven magnetic skyrmion motion, *Nat. Commun.* **15**, 1018 (2024).